

---

# CONTRASTIVE LANGUAGE–STRUCTURE PRE-TRAINING DRIVEN BY MATERIALS SCIENCE LITERATURE

---

Yuta Suzuki<sup>1</sup> Tatsunori Taniai<sup>2</sup> Ryo Igarashi<sup>2</sup> Kotaro Saito<sup>3,4</sup> Naoya Chiba<sup>5</sup>  
Yoshitaka Ushiku<sup>2</sup> Kanta Ono<sup>4</sup>

<sup>1</sup>Toyota Motor Corporation <sup>2</sup>OMRON SINIC X Corporation <sup>3</sup>Randeft, Inc.  
<sup>4</sup>Osaka University <sup>5</sup>Tohoku University

## ABSTRACT

Understanding structure–property relationships is an essential yet challenging aspect of materials discovery and development. To facilitate this process, recent studies in materials informatics have sought latent embedding spaces of crystal structures to capture their similarities based on properties and functionalities. However, abstract feature-based embedding spaces are human-unfriendly and prevent intuitive and efficient exploration of the vast materials space. Here we introduce Contrastive Language–Structure Pre-training (CLaSP), a learning paradigm for constructing crossmodal embedding spaces between crystal structures and texts. CLaSP aims to achieve material embeddings that 1) capture property- and functionality-related similarities between crystal structures and 2) allow intuitive retrieval of materials via user-provided description texts as queries. To compensate for the lack of sufficient datasets linking crystal structures with textual descriptions, CLaSP leverages a dataset of over 400,000 published crystal structures and corresponding publication records, including paper titles and abstracts, for training. We demonstrate the effectiveness of CLaSP through text-based crystal structure screening and embedding space visualization.

## 1 Introduction

The properties of materials, ranging from low-level properties such as bandgap and formation energy to high-level functionalities such as superconductivity, are determined by their crystal structures [1, 2]. Thus, unlocking the structure–property relationships of materials is key to accelerating materials discovery and development.

AI-driven materials science pursues this ambition through the use of machine learning (ML). One area of research has focused on predicting material properties using graph neural networks [3, 4, 5, 6] and transformers [7, 8], leveraging large-scale crystal structure datasets annotated with properties simulated by first-principles calculations. Although this approach has shown success, these models are specialized for specific simulatable properties, such as bandgap, and are unable to provide a comprehensive view of materials with diverse properties and functionalities.

Other studies have explored developing embedding spaces for crystal structures to capture their similarities based on properties and functionalities [9, 10, 11, 12]. However, these efforts are bottlenecked by the lack of dedicated training datasets with diverse property and functionality annotations. Annotating crystal structures is costly, requiring expert knowledge, physical experimentation, or computationally intensive simulations. Consequently, these methods often produce abstract, unannotated embedding spaces that are not easily navigable for materials discovery.

The annotation costs and model interpretability are common problems in ML, leading to the exploration of learning paradigms that use natural language text descriptions, instead of class labels, for supervision. The seminal work, CLIP (Contrastive Language–Image Pre-Training) [13], pioneered this approach by using contrastive learning between image and description text pairs. By learning to align two embedding spaces across the two modalities, CLIP enables crossmodal retrieval between images and texts, and zero-shot recognition of images using text-based prompts.

The success of CLIP has inspired language-supervised representation learning for molecules [14, 15, 16, 17, 18, 19] and materials [20, 21]. However, these methods for materials use textual descriptions about structural features rather than properties [20, 21], thus limiting their ability to capture high-level information such as material functionalities.

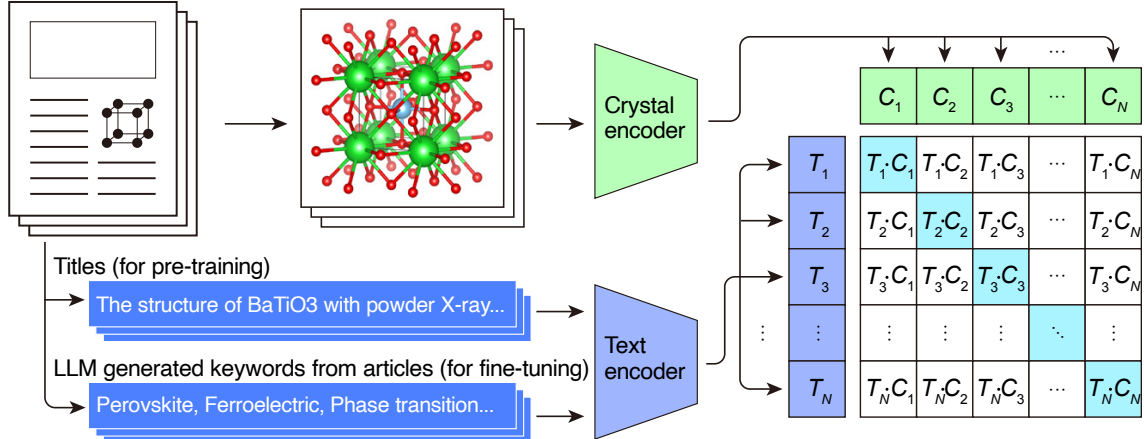


Figure 1: **Contrastive learning paradigm of CLaSP in two stages.** (1) Pre-training using pairs of crystal structures and publication titles. (2) Fine-tuning using pairs of crystal structures and keywords that are generated from the titles and abstracts using an LLM.

To overcome this limitation, we introduce Contrastive Language–Structure Pre-training (CLaSP) (Fig. 1). CLaSP leverages a large-scale dataset of published crystal structures and corresponding article information retrieved from the Crystallography Open Database (COD) [22]. Specifically, we utilize publication titles for pre-training and keyword-based captions, generated from pairs of titles and abstracts using a large language model (LLM), for fine-tuning.

We hypothesize that these textual sources provide a comprehensive representation of material characteristics. By leveraging bibliographic data as natural descriptions of structures, we bypass the need for labor-intensive, specialized annotations, enabling large-scale training of crossmodal models. The effectiveness of CLaSP is demonstrated through two key applications: intuitive text-based material retrieval and materials space mapping. Extensive analyses show that CLaSP effectively learns structure embeddings that capture abstract and complex material concepts, such as ‘superconductor’ and ‘metal-organic frameworks’.

## 2 Contrastive language–structure pre-training

We propose using a dataset of crystal structures paired with their publication information, such as titles and abstracts, for language–structure contrastive learning. By assuming that these texts convey material characteristics, this approach aims to link crystal structure embeddings with material properties and functionalities through human-interpretable linguistic semantics.

We used a total of 406,048 crystal structures associated with paper titles retrieved from the COD, as detailed in Sec. 7.2. CLaSP uses these captioned structures to jointly train a crystal encoder and a text encoder. For each training iteration, the crystal encoder transforms a batch of crystal structures into embeddings  $\{\mathbf{c}_i\}$ , whereas the text encoder transforms the paired caption texts into embeddings  $\{\mathbf{t}_i\}$ . This training procedure is outlined in Fig. 1. CLaSP aligns the two encoders by minimizing the large margin cosine loss function [23]:

$$L = -\frac{1}{N} \sum_{i=1}^N \log \frac{\exp(s(\cos(\mathbf{c}_i, \mathbf{t}_i) - m))}{\exp(s(\cos(\mathbf{c}_i, \mathbf{t}_i) - m)) + \sum_{j=1, j \neq i}^N \exp(s \cos(\mathbf{c}_i, \mathbf{t}_j))}, \quad (1)$$

which essentially increases the positive-pair similarities  $\cos(\mathbf{c}_i, \mathbf{t}_i)$  (*i.e.*, diagonal elements of the affinity matrix in Fig. 1) while reducing the negative-pair similarities  $\cos(\mathbf{c}_i, \mathbf{t}_j)$  (*i.e.*, off-diagonal elements).

Here,  $N$  is the batch size. The scaling hyperparameter  $s > 0$  amplifies cosine similarities to make the loss function more sensitive to small similarity differences, thereby enhancing training effectiveness. The margin hyperparameter  $m \in [0, 1]$  enforces a gap between the positive-pair similarities and the negative-pair similarities. This loss function is equivalent to the cross entropy loss in CLIP [13] when  $m = 0$ . We found that incorporating the margin leads to better generalization in downstream tasks, as we will show in Sec. 4.2.

To learn crystal embeddings  $\{\mathbf{c}_i\}$ , a CGCNN model [3] was trained from scratch to serve as the crystal encoder. For text embeddings  $\{\mathbf{t}_i\}$ , a frozen pre-trained SciBERT model [24] was used as the text encoder, followed by a three-layer

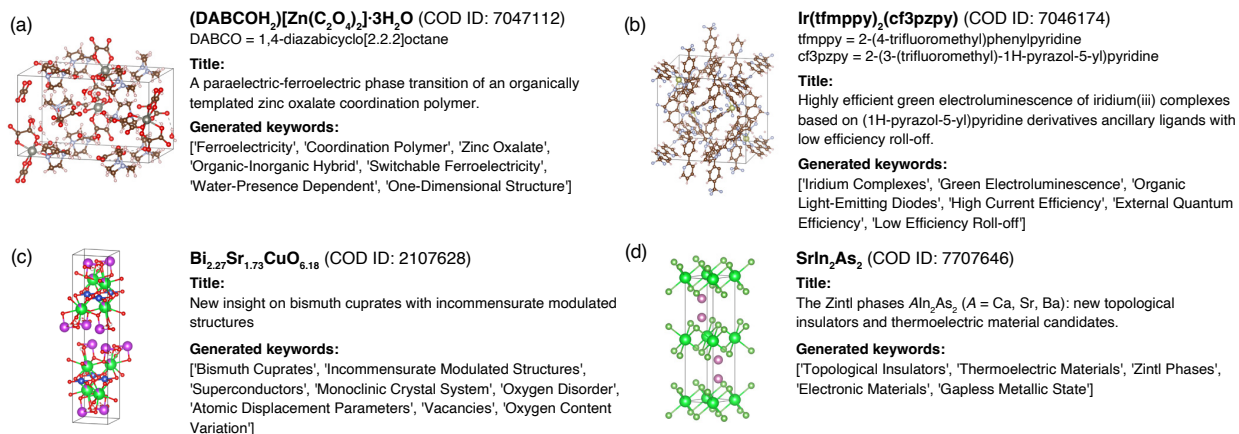


Figure 2: **Example of crystal structures with publication titles and generated keywords.** Panels (a)–(d) showcase dataset entries [26, 27, 28, 29] whose titles or keywords contain ‘ferroelectric’, ‘electroluminescence’, ‘superconductor’, and ‘thermoelectric’, respectively.

multilayer perceptron (MLP) fed with the CLS token embedding. We used the embedding dimensionality of 768 for both modalities. We provide the detailed training procedure in Sec. 7.1.

We consider keyword-based crystal structure screening as a demonstrative downstream task and hence perform fine-tuning using keyword captions instead of titles. To this end, we identified abstracts for 80,813 entries of the training set and generated keywords for these entries from their title–abstract pairs using an LLM. We used Meta’s Llama 3 [25] to generate up to 10 keywords, such as ‘visible light photocatalysis’ and ‘narrow bandgap’, for each crystal structure. Examples of dataset entries are displayed in Fig. 2, and the overall dataset generation procedure is detailed in Sec. 7.2–7.4.

### 3 Related work

Our work builds upon several lines of research in materials informatics, ML, and natural language processing (NLP). Below, we briefly review these studies and discuss their relevance and differences with our approach.

#### 3.1 Crystal structure modeling

Crystal structure modeling using neural networks serves as a fundamental basis for ML models that process crystal structures. One of its most straightforward applications is crystal property prediction, for which various crystal encoder architectures have been proposed. These architectures typically employ geometric graph neural networks (GNNs) that model interatomic interactions via neural message passing. Early successful examples include CGCNN [3] and SchNet [30], which represent crystal structures as distance-based graphs. Subsequent work has aimed to capture richer interaction representations by incorporating bond and global state attributes [4], three-body interactions [31], attention mechanisms [32, 7, 8], and infinite periodicity [6, 8].

These GNN models demonstrate high accuracy in predicting specific properties, such as bandgap and formation energy. However, they all rely on the availability of large-scale datasets (*e.g.*, the Materials Project [33] and JARVIS-DFT [34]) with property labels simulated by first-principles calculations for training. As a result, these approaches face challenges when applied to domains where training data are limited or poorly curated. They are also restricted to predicting specific target properties rather than capturing the comprehensive characteristics of materials.

More recent work focuses on developing surrogate models for interatomic potentials [5, 35, 36, 37], rather than targeting specific properties. However, like earlier approaches, these models also depend on large-scale training datasets with simulated property labels, such as the Materials Project [33] or the Open Catalyst Dataset [38, 39].

In our work, we introduce a novel learning paradigm for crystal structure modeling by leveraging language supervision from publication records. This approach enables the model to learn diverse material characteristics—ranging from bandgap to superconductivity—without requiring explicitly labeled training data. To demonstrate this approach, we adopt CGCNN [3] as the crystal encoder for its simplicity and established recognition as a baseline model. The high

efficiency of CGCNN is particularly important for our COD dataset, which consists of over 400,000 structures with an average of about 190 atoms per material.

### 3.2 Embedding learning for materials and crystal structures

Embedding learning is another actively explored application of crystal structure modeling, aimed at understanding the materials space by capturing property- and functionality-level similarities. Early studies focused on learning atom representations for limited material classes (*e.g.*, alkali metals and metalloids) [9, 40, 41]. For example, Xie *et al.* [9] derived atom embeddings by utilizing latent features from a GNN trained on a property prediction task.

To learn more comprehensive material representations on a large scale, Suzuki *et al.* [10] proposed a global mapping of 120k diverse materials via self-supervised contrastive learning between crystal structures and diffraction patterns. Remarkably, their embedding space reportedly captured complex material concepts, such as superconductors and lithium-ion battery materials, without requiring annotated training data. Li *et al.* [11] investigated similar global mappings using various material fingerprint representations in a property prediction pre-training approach.

However, these embedding approaches often lack interpretability for humans, as the meaning of individual dimensions within the learned embedding vectors is difficult to discern. Because of this, Suzuki *et al.* [10] relied on a query structure with known properties to retrieve materials with similar properties. This limitation underscores the growing need for more intuitive and interpretable methods to facilitate functionality-driven materials exploration and design.

More recent studies have explored extending material representations through multimodal learning with texts [20, 21], aiming to attribute semantic meaning to material embeddings. For example, Ozawa *et al.* [21] used crystal structures along with rule-based textual descriptions of their geometric features for contrastive learning. However, these methods rely on textual descriptions of structural features rather than material properties, thus limiting their ability to capture high-level information such as material functionalities.

In our work, we demonstrate that publication records in the materials science literature can effectively teach models about the complex properties of associated structures, by leveraging advances in language modeling discussed below.

### 3.3 Language modeling and multimodal learning

Our study leverages language modeling for its three crucial roles in ML applications utilizing textual data: machine understanding, human interpretation, and language supervision.

Historically, a primary goal of ML-based language modeling has been to enable machines to understand textual information. For instance, word2vec [42] was proposed to learn semantic vector representations of words from their co-occurrences in texts, and seq2seq models [43, 44] enabled context-aware translation and summarization. In particular, the transformer architecture [44] excels at parallel computation and capturing long-range dependencies. This innovative architecture has fueled large-scale self-supervised pre-training of language models [45], driving significant progress in machine text understanding and ultimately leading to the advent of LLMs with impressive capabilities, such as the GPT [46, 47, 48, 49] and Llama [50, 51, 25] series.

An early and notable application of these NLP methods in materials science was demonstrated by Tshitoyan *et al.* [52]. They applied word2vec [42] to a corpus of 3.3 million scientific abstracts from the materials science literature. Their findings showed that the learned word embeddings captured latent knowledge about materials science, including novel insights that were not explicitly presented in the used corpus. This suggests the potential for data-driven research through mining the massive body of scientific literature, as well as the informativeness of abstracts.

Our study builds on more recent advances in language modeling, specifically by adopting SciBERT [24] as the text encoder (Sec. 2) and utilizing Llama 3 [25] for keyword extraction from title-abstract pairs in dataset generation (Sec. 7.4). SciBERT is a variant of BERT [45] pre-trained on a large corpus of scientific publications, thus particularly suited for analyzing the bibliographic texts.

Since language is one of the most intuitive forms of information for humans, it is also useful to enhance the interpretability and interactivity of ML models through multimodal learning [13, 53]. As discussed in the previous section, our work and other recent studies [20, 21] employ contrastive learning between texts and structures to embed linguistic semantics into structural representations.

Furthermore, when powerful language models are integrated into this multimodal learning paradigm, they can derive strong supervision from noisy natural-language texts. As demonstrated by CLIP [13] and other studies [54, 53] on image data, this learning strategy treats natural language as a high-freedom annotation, eliminating the need for high-quality labeled datasets.

A major difference between our work and these computer vision applications [13, 54] is that, in computer vision, crowd-labeled datasets (e.g., ImageNet [55] and MS COCO [56]) are often available or affordable. In contrast, materials science lacks large-scale datasets that describe material properties and functionalities. This is primarily because annotating crystal structures requires expert knowledge or labor-intensive experimentation, making crowd-sourcing impractical. Our work addresses this issue by leveraging bibliographic records associated with structures as annotations, inspired by the word2vec approach of Tshitoyan *et al.* [52].

## 4 Results

In this section, we demonstrate the effectiveness of the proposed approach both quantitatively and qualitatively through two applications: text-based material retrieval and embedding space visualization. For text-based material retrieval (Sec. 4.1), we evaluate how accurately the model links crystal structures with their textual descriptions, such as ‘superconductor’ and ‘narrow-bandgap material’. Additionally, we verify the design of our loss function through this retrieval application (Sec. 4.2). For embedding space visualization, we construct an intuitive map of the materials space (Sec. 4.3) and compare it with an existing embedding approach (Sec. 4.4).

### 4.1 Zero-shot crystal structure screening by texts

To evaluate CLaSP’s ability to link crystal structures with textual property descriptions, we performed crystal structure retrieval using keywords representing material functionalities (e.g., ‘thermoelectric’ and ‘superconductor’). Given the embedding of a query keyword, we retrieved structure embeddings from the test set that showed high cosine similarities with the keyword embedding. We regarded a structure to possess a queried property if the associated paper title contained the keyword or its variations (e.g., given ‘superconductor’ as a query, the terms ‘superconductive’ and ‘superconductivity’ were also considered correct).

We evaluated the trade-off between true positives and false positives using the ROC (receiver operating characteristic) and ROC-AUC (area under the ROC curve). Additionally, we assessed Average Precision (AP). Given the extremely low positive-to-negative ratios in our retrieval tasks (*i.e.*, 20 to 165 positives in a total of 40,604 samples for each keyword), we evaluated AP using a balanced random subset of negative samples to make the AP scores more informative.

Figure 3 shows ROC curves for six query keywords before and after fine-tuning, with dashed diagonal lines representing random selection. For a more comprehensive evaluation, Table 1 summarizes the mean and individual ROC-AUC scores for the six keywords, along with the Average Precision (AP) scores. While the zero-shot prediction using the pre-trained model (Fig. 3, left) already demonstrates good performance, with a mean ROC-AUC of 0.7185, fine-tuning (Fig. 3, right) further improved it to 0.7804. A similar trend is observed in the AP evaluation (Table 1). These results highlight the ability of the CLaSP model to capture complex structure–property relationships across diverse material functionalities by analyzing crystal structures alone. Section 5 will discuss these findings in more detail.

To further validate the retrieval performance, we retrieved the top-100 materials using keywords related to bandgap—specifically, ‘narrow-bandgap material’ and ‘insulator’—and analyzed their bandgap distributions. Since the COD does not provide property labels, we predicted bandgaps of materials by using a state-of-the-art property prediction model, Crystalformer [8], with pre-trained model weights (specifically the seven-block model trained on the JARVIS-DFT 3D 2021 dataset) provided by the authors.

Figure 4 shows violin plots of the bandgaps for the retrieved materials. These distributions successfully reflect the expected bandgap ranges for narrow-bandgap materials (*i.e.*, bandgaps smaller than 1.1 eV) and insulators (*i.e.*, large bandgaps), compared to the random sampling distribution.

### 4.2 Verification of loss function design

Through this keyword-based retrieval task, we also investigated the impact of loss function design (Eq. 1), which was adapted from CosFace [23] instead of CLIP [13]. Specifically, we analyzed how the model’s performance depends on the margin and scale hyperparameters in the loss function, coincides with CLIP’s loss when the margin is set to zero. We trained the model with various combinations of margin  $m \in \{0, 0.3, 0.5\}$  and scale  $s \in \{1.0, 1.5, 2.0, 2.5, 3.0, 3.5\}$ , and evaluated the mean ROC-AUC scores both before and after fine-tuning.

The results in Table 2 indicate that both parameters impact performance. Particularly, a higher margin tends to increase validation scores after fine-tuning, suggesting that the margin loss promotes better generalization in downstream tasks.

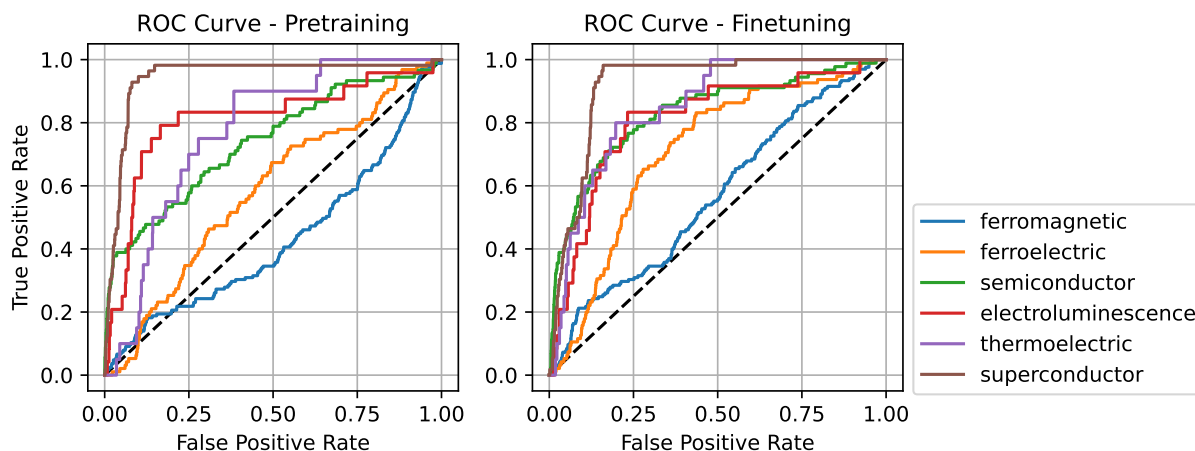


Figure 3: **ROC curves of keyword-based crystal structure retrieval.** The zero-shot results with only pre-training (left) show good performance, and fine-tuning leads to further improvements (right). The test set consists of 40,604 materials, and the dashed diagonal lines represent the ROC curves for random selection.

Table 1: **ROC-AUC and Average Precision (AP) scores for keyword-based crystal structure retrieval.** ROC-AUC was evaluated on the entire test set (40,604 materials), while AP was evaluated on a balanced subset with randomly subsampled negatives. PT and FT stand for pre-trained and fine-tuned scores, respectively. The numbers in **bold** indicate the best scores.

Query	# Positives	ROC-AUC		AP	
		PT	FT	PT	FT
ferromagnetic	165	0.4281	0.5674	0.5018	0.5716
ferroelectric	95	0.5814	0.7097	0.5357	0.6380
semiconductor	90	0.7382	0.8290	0.7705	0.8254
electroluminescence	24	0.8106	0.8090	<b>0.9050</b>	0.8759
thermoelectric	20	0.7714	0.8496	0.7987	<b>0.9124</b>
superconductor	56	<b>0.9431</b>	<b>0.9180</b>	0.8880	0.8228
Avg.	-	0.7121	0.7804	0.7333	0.7743

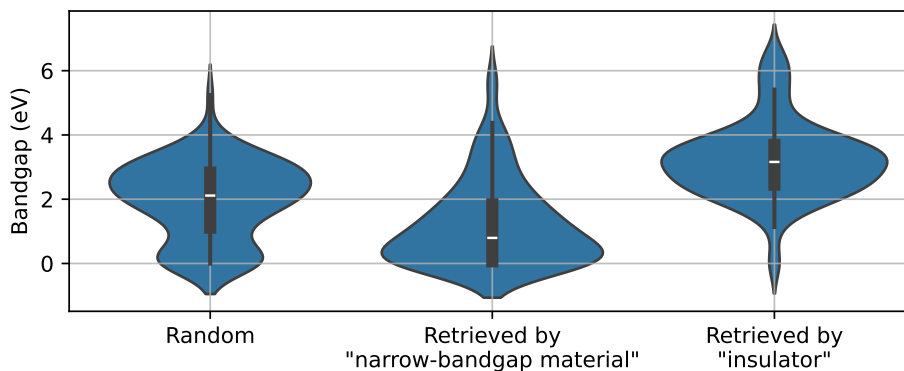


Figure 4: **Violin plots of bandgaps for crystals retrieved via keyword searches.** The distributions reflect the expected bandgap ranges for narrow bandgap materials and insulators, successfully demonstrating the retrieval of materials with targeted properties.

Table 2: **ROC-AUC comparison of keyword-based crystal structure retrieval across different loss hyperparameters.** The numbers in **bold** indicate the best results and the numbers with underline indicate the second best results.

Loss	Margin	Scale	Pre-trained (val)	Fine-tuned (val)
CLIP [13]	0.0	1.0	0.6310	0.6943
	0.0	1.5	0.6526	0.6521
	0.0	2.0	0.7152	0.7336
	0.0	2.5	0.6553	0.6791
	0.0	3.0	0.6946	0.7227
	0.0	3.5	0.6053	0.6856
CosFace [23]	0.3	1.0	0.5156	0.6495
	0.3	1.5	<u>0.7170</u>	0.7273
	0.3	2.0	0.6074	0.6701
	0.3	2.5	0.6925	0.7365
	0.3	3.0	0.6223	0.7395
	0.3	3.5	0.6498	0.7496
	0.5	1.0	0.6282	0.6994
	0.5	1.5	0.7164	0.7763
	0.5	2.0	0.5832	0.7006
	0.5	2.5	0.6347	<u>0.7778</u>
	0.5	3.0	<b>0.7185</b>	<b>0.7828</b>
0.5	3.5	0.6764	0.7031	

### 4.3 Embedding space visualization

To demonstrate how the proposed language–structure embedding can intuitively navigate the materials space, we created several visualizations of the structure embeddings from the test set using t-SNE.

First, we created a *world map* of COD materials to analyze the alignment of the learned materials space and semantics. We grouped the structure embeddings into 20 clusters using k-means++ and assigned each cluster an LLM-generated keyword label that summarizes the associated paper titles, as detailed in Sec. 7.5.

The resulting map in Fig. 5a shows a meaningful distribution of materials, forming lands of clusters of similar materials, such as an organic materials land, a complexes land, and an inorganic materials land. The map suggests that the model recognizes material similarities that are intuitive to human. In contrast, embeddings learned without textual information often fail to capture such high-level semantic relationships, as we will show in the next section.

Furthermore, cosine similarity-based heat maps allow us to easily identify regions relevant to a given text query. Figure 5b shows that ‘superconductor’ is highly correlated with intermetallic compounds and oxides, while Fig. 5c shows ‘metal-organic frameworks’ is aligned with organic compounds.

Finally, we verified the alignment of the map constitution with material properties by overlaying predicted properties onto the map. As done in Sec. 4.1, we used the pre-trained Crystalformer [8] to predict the bandgaps of the COD materials. The resulting bandgap distribution in Fig. 5d shows consistencies with the map (Fig. 5a). For example, the right part in Fig. 5d with larger bandgaps corresponds to organic compounds in Fig. 5a, and the bottom part with near-zero bandgaps corresponds to intermetallic compounds. These results suggest that the embeddings not only capture intuitive semantics of materials but also reflect their similarities in terms of material properties.

### 4.4 Comparison with an existing approach

We compared CLaSP with an existing crystal embedding learning approach called Contrastive Materials Metric Learning (CMML) [10]. CMML also employs contrastive learning, but it aligns the embeddings of two complementary structural representations: crystal structures and their corresponding X-ray diffraction (XRD) patterns. Since XRD patterns can be easily simulated from crystal structures, CMML enables self-supervised learning that only requires a collection of unannotated crystal structures for training.

However, unlike CLaSP, which aligns structure–language pairs, CMML uses pairs of purely structural data (*i.e.*, structure and XRD patterns). As a result, CMML produces abstract embeddings that limit human-intuitive understanding, and it also prevents a quantitative comparison in the text-based retrieval task (Sec. 4.1).



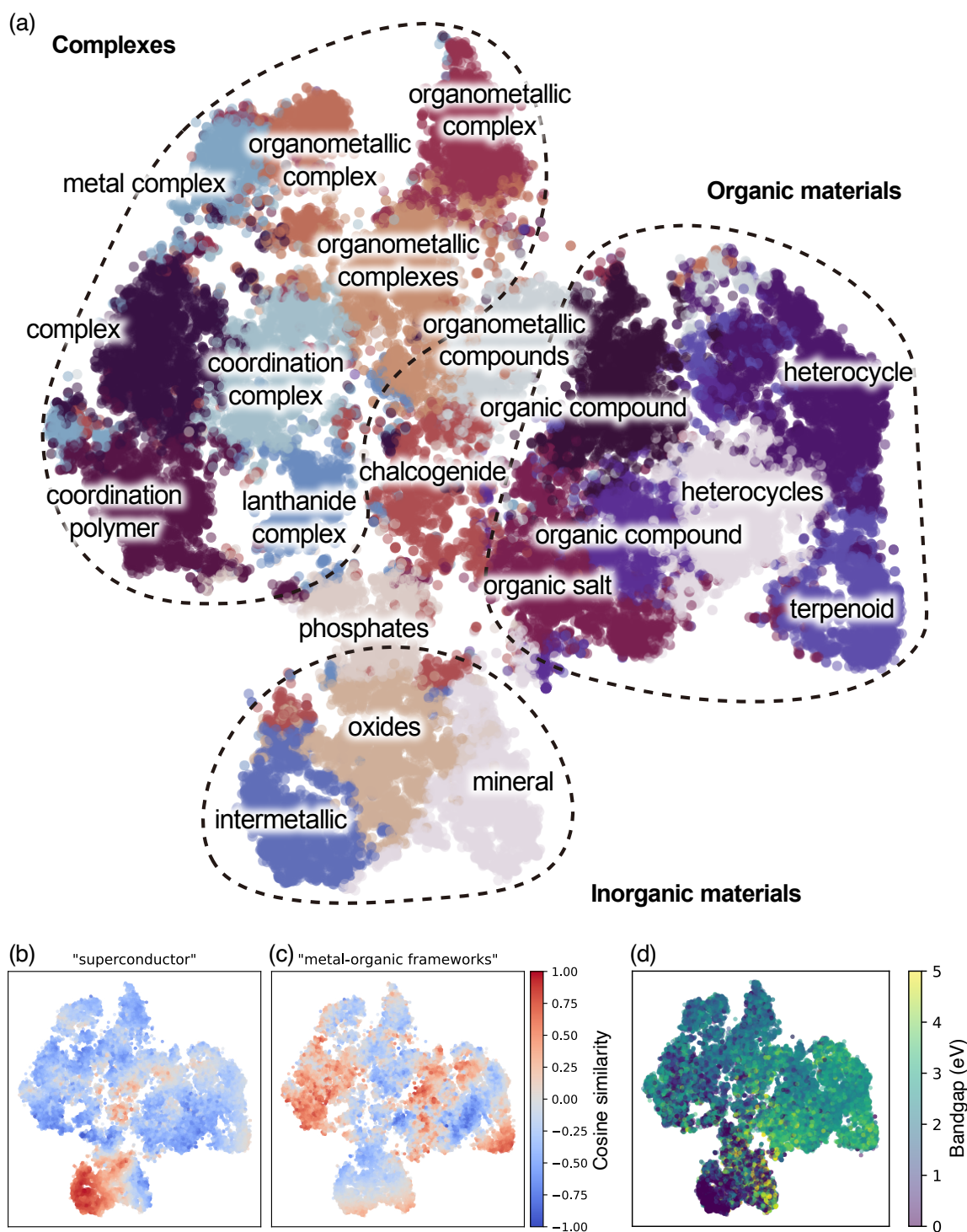


Figure 5: **t-SNE visualization of crystal structure embeddings.** (a) *World map* of COD materials. The embeddings are grouped into 20 clusters and assigned keywords that represent the paper titles associated with the clusters. (b, c) Heat maps showing cosine similarities between the structure embeddings and query-text embeddings ('superconductor' and 'metal-organic frameworks'). (d) Bandgap distribution of crystal structure embeddings. Predicted bandgaps trend to reflect known properties of material clusters in (a), such as larger bandgaps for organic compounds and near-zero bandgaps for intermetallic compounds.



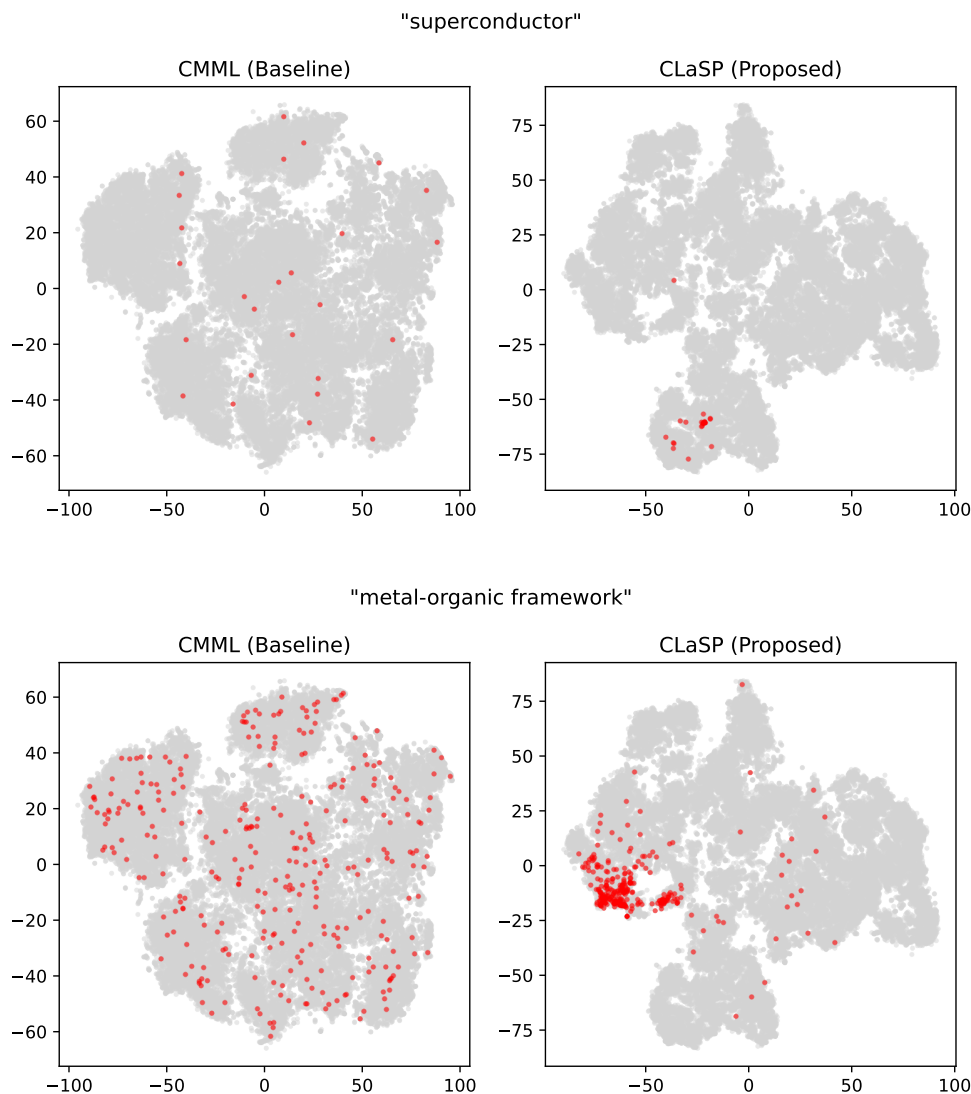


Figure 6: **t-SNE visualizations of crystal structure embeddings comparing CMML [10] and CLaSP.** Material entries with publication titles that include the keywords ‘superconductor’ (top row) or ‘metal-organic framework’ (bottom row) are highlighted in red.

To compare how well these two approaches capture the high-level semantics of materials, we visually examined how they map semantically similar materials in their respective embedding spaces. Specifically, we generated embeddings of the crystal structures in the COD test set using both the CLaSP model and the CMML model (pre-trained on the Materials Project dataset) that is publicly provided by the authors. We then created t-SNE visualizations of these embeddings, highlighting entry points whose corresponding publication titles included specific keywords—specifically, ‘superconductor’ and ‘metal-organic framework.’

The comparisons in Fig. 6 show that, while CMML randomly scatters these keyword-specified entries across the map (left), CLaSP highly concentrates them in specific areas in the map (right). These concentrated areas also align with the areas of intermetallic compounds and organic compounds in the materials map in Fig. 5a.

These results highlight a key advantage of CLaSP. By incorporating textual information during training, CLaSP learns to recognize similarities between materials based not only on their structures but also on their properties and functionalities through text-based supervision. In contrast, CMML, which relies solely on structural data, struggles to capture these high-level relationships among materials, particularly when they exhibit diverse structures or compositions.

## 5 Discussion and limitations

### 5.1 Use of titles and abstracts for supervision

Both the screening and visualization results in Sec. 4 have confirmed that publication information provides strong supervision for learning crystal structure embeddings and linking them to material properties.

However, titles in the materials science literature tend to highlight specific, potentially intriguing aspects of the reported materials, rather than offering a comprehensive description. For example, in Fig. 3a and Table 1 (PT), the ROC performance for the keyword ‘superconductor’ outperforms that for ‘semiconductor’ and other keywords, despite the more complex structure–property relationships involved. We hypothesize that this is due to the frequent co-occurrence of superconductivity in the materials and the term ‘superconductor’ in the titles, whereas ‘semiconductor’ is less prioritized.

A similar issue may explain the relatively low retrieval accuracy for the keyword ‘ferromagnetic’ in Fig. 3a and Table 1 (PT). Since ferromagnetism is a major characteristic of widely used iron-based materials, paper titles often omit the term ‘ferromagnetic.’ This could introduce noise into the title-based supervision and hinder the learning of this material concept. In contrast, Fig. 3b and Table 1 (FT) show that fine-tuning using keywords derived from both titles and abstracts improves the overall retrieval performance. This suggests that abstracts convey more comprehensive information about the materials.

These results suggest potential improvements for CLaSP by incorporating richer training data sources beyond publication titles and abstracts, such as full texts, figures, and tables. Additionally, when papers cite other publications that report specific crystal structures, the citation contexts may provide valuable text descriptions for those structures.

### 5.2 Dataset biases

Our analysis also revealed a potential bias in the COD dataset, which is predominantly composed of crystallography and chemistry publications. Over 80% of the entries come from a small subset of journals primarily focused on these fields (Fig. 7). This bias is understandable, given the COD’s historical development and its emphasis on crystallography. However, it highlights the need for more diverse data sources to ensure a comprehensive representation of materials and their properties. Given the limited availability of large materials databases with publication records beyond the COD, augmentation with external sources, such as citation contexts and Wikipedia entries, could be beneficial. This approach is similar to retrieval-augmented generation (RAG) [57] used in LLM applications. We leave such extensions for future work.

## 6 Conclusions and broader impacts

In this study, we introduced CLaSP, a literature-driven learning paradigm for constructing crossmodal embedding spaces that connect crystal structures with their textual property descriptions. We demonstrated its effectiveness in learning structure embeddings that capture functionality-level material similarities and in enhancing the materials space with intuitive linguistic semantics.

These promising results indicate the potential to transform how we explore the vast materials space. Potential applications include crystal structure screening and tagging via text prompts. Furthermore, inspired by text-to-image generation [58], CLaSP’s text embeddings could guide crystal structure generation models [59, 60], enabling innovative applications such as text-to-crystal generation. These advancements promise a more intuitive and efficient approach to exploring the materials space.

## 7 Method details

Below, we provide detailed procedures for model training, dataset creation, and embedding visualization.

### 7.1 Training settings

We optimized the loss function in Eq. 1 with scaling factor  $s$  of 3 and margin  $m$  of 0.5, using stochastic gradient descent with global batch size  $N$  equal to 16,384 ( $2,048 \times 8$  GPUs). Title-based pre-training was performed for a total of 2000 epochs, followed by keyword-based fine-tuning for additional 50 epochs. We used the AdamW optimizer [61, 62] with a constant learning rate of  $2 \times 10^{-5}$  for pre-training and  $1 \times 10^{-6}$  for fine-tuning. The networks and training code

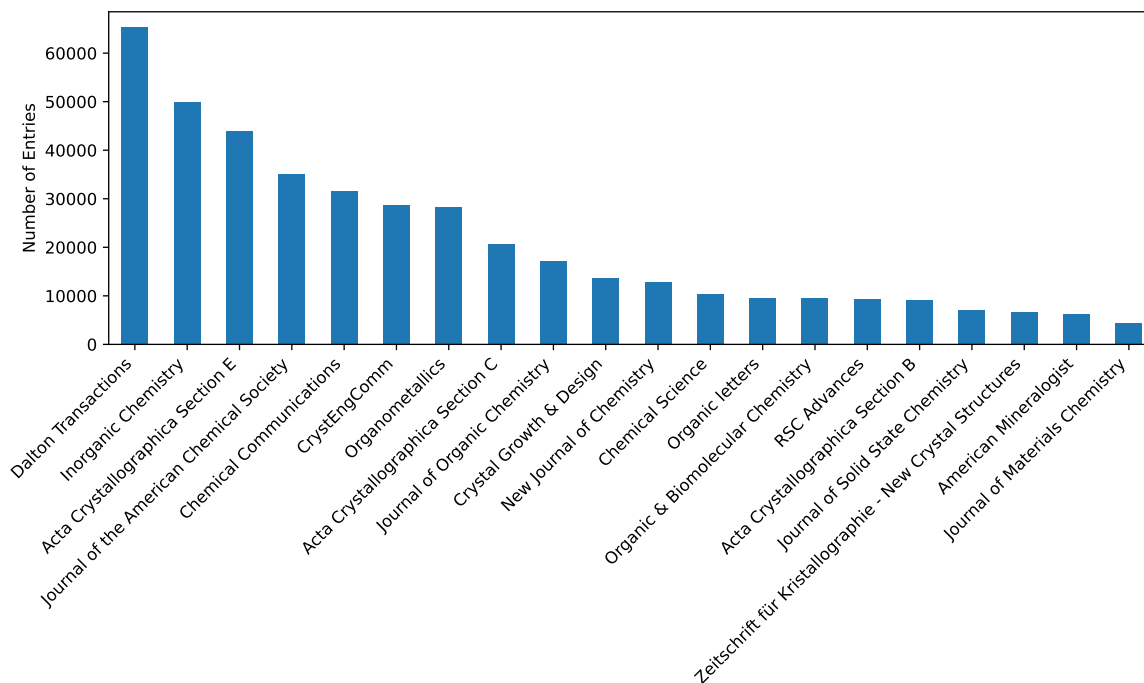


Figure 7: **Top 20 journals contributing to the COD dataset.**

were implemented in Python using PyTorch [63] and PyTorch Geometric [64]. Training was performed on a single server with eight NVIDIA A100 GPUs (80GB VRAM), taking approximately 16 hours overall.

## 7.2 Data retrieval

This study used the Crystallography Open Database (COD) [22] as the source of crystal structure data. Compared to other crystal structure databases, the COD is particularly well-suited for our purposes, as it provides publication information (including titles and DOIs) for each crystal structure entry and is available in the public domain.

From the COD, we retrieved 512,312 pairs of crystal structures and their corresponding publication records as of March 2024. Using the DOIs from these records, we further extracted the abstracts of the papers via the Crossref API. This process collected abstracts for 141,311 entries, representing approximately 27.6% of the entire dataset.

## 7.3 Data preprocessing and splitting

We filtered out the entries with structures containing more than 500 atomic sites, resulting in a dataset of 406,048 crystal structures with corresponding paper titles and DOIs. We randomly split the dataset into training, validation, and test sets in an 8:1:1 ratio, yielding 324,838 entries for training, 40,604 for validation, and 40,606 for testing.

We used the train set for title-based pre-training, the validation set for selecting a model checkpoint during pre-training or fine-tuning, and the test set for evaluating the retrieval performance (Figs. 3 and 4; Table 1) and for visualizing the embedding space (Figs. 5 and 6). We also used this dataset to generate the keyword-captioned dataset for fine-tuning, as explained next.

## 7.4 Keyword dataset generation for fine-tuning

We derived the keyword-captioned dataset from the main dataset by removing entries without abstract from each split, ensuring no mixing across the splits. For each entry with a title and abstract pair, we generated up to 10 representative keywords using an LLM, specifically Meta’s Llama 3 (70B Instruct) [25]. The prompt template used for keyword generation is listed below.

The keyword generation process took 36 hours using a server equipped with eight NVIDIA A100 GPUs (80GB VRAM) and an efficient LLM inference framework, vLLM [65]. Finally, we removed generated keywords if they were unrelated

to material properties, such as ‘crystal structure’, ‘X-ray diffraction’, ‘neutron diffraction’, ‘powder diffraction’, and ‘single-crystal X-ray diffraction’. Entries without any remaining keywords were also removed from the dataset.

This process resulted in 80,813 entries for the training set, which was used to fine-tune the pre-trained model for the keyword-based retrieval task. The remaining two sets, containing 10,134 entries for validation and 10,197 for testing, were never used in this study. Note that the validation during fine-tuning was done based on the mean ROC-AUC score, instead of the validation loss, for the validation set of the main dataset.

```
def prompt_format_func(material_id, title, abstract):
    return \
    f"""Below are title-abstract pairs for materials science papers dealing with crystal structures. For each paper, list up
    ↪ to 10 keywords in English that describe the features, functions, or applications of the material discussed. Focus
    ↪ on the material itself, and do not include general terms or measurement techniques (e.g., Crystal Structure,
    ↪ Crystal Lattice, X-ray diffraction, Neutron Diffraction, Powder Diffraction). Return the results in json format
    ↪ with the following schema.

    **Example input 1:**
    """
    ID: 0001
    Title: Enhancement of Critical Temperature in Layered Copper Oxide Superconductors via Lattice Compression Techniques
    Abstract: Superconductivity in copper oxides (cuprates) offers vast potential for technological applications due to their
    ↪ high critical temperatures (Tc). Our research presents a novel approach to enhance Tc in layered cuprate materials
    ↪ through the controlled application of lattice compression. Using advanced crystallographic methods, we
    ↪ systematically altered the interlayer spacing and analyzed the resultant changes in electronic properties. Our
    ↪ findings demonstrate a significant improvement in superconducting behavior at elevated temperatures, further
    ↪ supporting the unconventional mechanisms underpinning superconductivity in these materials.
    """

    **Example output 1:**
    """json
    [{"ID": "0001",
     "Keywords": ["High-Tc", "Cuprate Superconductors", "Lattice Compression", "Electronic Properties", "Layered Structures",
     ↪ "Superconducting Phase", "Temperature Enhancement", "Unconventional Superconductivity"]}
    ]
    """

    **Example input 2:**
    """
    ID: 0002
    Title: Advancements in Biodegradable Polymers for Sustained Drug Delivery Systems
    Abstract: The development of biocompatible and biodegradable materials is critical in the field of medical implants and
    ↪ drug delivery systems. This paper examines the latest advancements in biodegradable polymers tailored for
    ↪ sustained release of therapeutic agents. We analyze various polymer compositions that provide controlled
    ↪ degradation rates and compatibility with a range of drugs. Our results show promising applications in long-term
    ↪ treatments, reducing the need for repeated administration and improving patient compliance.
    """

    **Example output 2:**
    """json
    [{"ID": "0002",
     "Keywords": ["Biomaterials", "Biodegradable Polymers", "Sustained Release", "Drug Delivery Systems", "Biocompatibility",
     ↪ "Controlled Degradation", "Therapeutic Agents", "Medical Implants", "Long-Term Treatment"]}
    ]
    """

    **Input **:
    """
    ID: {material_id}
    Title: {title}
    Abstract: {abstract}
    """

    **Output **:
    """json
    """
```

## 7.5 Visualizations

Crystal structures in Figs. 1 and 2 were visualized using VESTA [66]. For the embedding space visualizations shown in Figs. 5 and 6, we employed the t-SNE algorithm [67], as implemented in openTSNE [68]. In Fig.5, embedding clusters were generated using the k-means++ algorithm [69]. These clusters were further annotated by summarizing the associated paper titles using Google Gemini 1.5 Pro with a default temperature parameter of 1.0.

## Acknowledgments

R. I. is partly supported by JSPS KAKENHI Grant Number 24K23910. N. C. is partly supported by JSPS KAKENHI Grant Number 21K14130. Y. U. is partly supported by JST-Mirai Program Grant Number JPMJMI21G2 and JST Moonshot R&D Program Grant Number JPMJMS2236.

## Data availability

This study used the Crystallography Open Database (COD) [22] as the source of crystal structure data. Please see Sec. 7.2–7.4 for the data retrieval and processing details.

## Code availability

We will release our code upon acceptance of this work for publication.

## Author contributions

YS conceived the concept, developed the model, conducted the analysis, and drafted the manuscript. TT provided guidance on the methodology, analysis and writing, assisted with the literature review, and revised the manuscript draft. RI and KS contributed expertise in materials science, advising on the analysis. NC contributed expertise in machine learning, advising on the methodology. YU co-led materials-related collaborations, provided guidance on the plan and methodology from a machine learning perspective, and advised on the writing. KO co-led materials-related collaborations and provided guidance on the plan and analysis from a materials science perspective.

## Conflict of interest

The author declares no competing interests.

## References

- [1] Callister, W. D. & Rethwisch, D. G. *Materials Science and Engineering* (John Wiley and Sons, 2010).
- [2] De Graef, M. & McHenry, M. E. *Structure of Materials. An Introduction to Crystallography, Diffraction and Symmetry* (Cambridge University Press, 2012).
- [3] Xie, T. & Grossman, J. C. Crystal Graph Convolutional Neural Networks for an Accurate and Interpretable Prediction of Material Properties. *Phys. Rev. Lett.* **120**, 145301 (2018). doi:10.1103/PhysRevLett.120.145301.
- [4] Chen, C., Ye, W., Zuo, Y., Zheng, C. & Ong, S. P. Graph Networks as a Universal Machine Learning Framework for Molecules and Crystals. *Chem. Mater.* **31**, 3564–3572 (2019). doi:10.1021/acs.chemmater.9b01294.
- [5] Chen, C. & Ong, S. P. A universal graph deep learning interatomic potential for the periodic table. *Nat. Comput. Sci.* **2**, 718–728 (2022). doi:10.1038/s43588-022-00349-3.
- [6] Lin, Y. *et al.* Efficient Approximations of Complete Interatomic Potentials for Crystal Property Prediction. In *The 40th International Conference on Machine Learning (ICML 2023)*, vol. 202 of *Proceedings of Machine Learning Research*, 21260–21287 (2023). Online: <https://proceedings.mlr.press/v202/lin23m.html>.
- [7] Yan, K., Liu, Y., Lin, Y. & Ji, S. Periodic Graph Transformers for Crystal Material Property Prediction. In *Advances in Neural Information Processing Systems 25 (NeurIPS 2022)*, 15066–15080 (2022). arXiv:2209.11807.
- [8] Taniai, T. *et al.* Crystalformer: Infinitely Connected Attention for Periodic Structure Encoding. In *The Twelfth International Conference on Learning Representations (ICLR 2024)* (2024). Online: <https://openreview.net/forum?id=fxQiecl9HB>.
- [9] Xie, T. & Grossman, J. C. Hierarchical visualization of materials space with graph convolutional neural networks. *J. Chem. Phys.* **149**, 174111 (2018). doi:10.1063/1.5047803.
- [10] Suzuki, Y., Taniai, T., Saito, K., Ushiku, Y. & Ono, K. Self-supervised learning of materials concepts from crystal structures via deep neural networks. *Mach. Learn.: Sci. Technol.* **3**, 045034 (2022). doi:10.1088/2632-2153/aca23d.

- [11] Li, Q. *et al.* Global Mapping of Structures and Properties of Crystal Materials. *J. Chem. Inf. Model.* **63**, 3814–3826 (2023). doi:10.1021/acs.jcim.3c00224.
- [12] Qu, J. *et al.* Leveraging language representation for materials exploration and discovery. *npj Comput. Mater.* **10**, 1–14 (2024). doi:10.1038/s41524-024-01231-8.
- [13] Radford, A. *et al.* Learning Transferable Visual Models from Natural Language Supervision. In *The 38th International Conference on Machine Learning (ICML 2021)*, vol. 139 of *Proceedings of Machine Learning Research*, 8748–8763 (2021). Online: <https://proceedings.mlr.press/v139/radford21a.html>.
- [14] Zeng, Z., Yao, Y., Liu, Z. & Sun, M. A deep-learning system bridging molecule structure and biomedical text with comprehension comparable to human professionals. *Nat. Commun.* **13**, 862 (2022). doi:10.1038/s41467-022-28494-3.
- [15] Wang, J. *et al.* Multi-modal chemical information reconstruction from images and texts for exploring the near-drug space. *Brief. Bioinform.* **23**, bbac461 (2022). doi:10.1093/bib/bbac461.
- [16] Liu, S. *et al.* Multi-modal molecule structure–text model for text-based retrieval and editing. *Nat. Mach. Intell.* **5**, 1447–1457 (2023). doi:10.1038/s42256-023-00759-6.
- [17] Seidl, P., Vall, A., Hochreiter, S. & Klambauer, G. Enhancing Activity Prediction Models in Drug Discovery with the Ability to Understand Human Language. *CoRR* (2023). arXiv:2303.03363.
- [18] Takeda, S. *et al.* Multi-modal Foundation Model for Material Design. In *The NeurIPS 2023 Workshop on AI for Accelerated Materials Design (AI4Mat 2023)* (2023). Online: <https://openreview.net/forum?id=EtT2bLsfM9>.
- [19] Kaufman, B. *et al.* COATI: Multimodal Contrastive Pretraining for Representing and Traversing Chemical Space. *J. Chem. Inf. Model.* **64**, 1145–1157 (2024). doi:10.1021/acs.jcim.3c01753.
- [20] Moro, V. *et al.* Multimodal Learning for Materials. *CoRR* (2024). arXiv:2312.00111.
- [21] Ozawa, K., Suzuki, T., Tonogai, S. & Itakura, T. Graph-text contrastive learning of inorganic crystal structure toward a foundation model of inorganic materials. *STAM Methods* **0**, 2406219 (2024). doi:10.1080/27660400.2024.2406219.
- [22] Gražulis, S. *et al.* Crystallography Open Database – an open-access collection of crystal structures. *J. Appl. Crystallogr.* **42**, 726–729 (2009). doi:10.1107/S0021889809016690.
- [23] Wang, H. *et al.* CosFace: Large Margin Cosine Loss for Deep Face Recognition. In *The 2018 IEEE/CVF Conference on Computer Vision and Pattern Recognition (CVPR 2018)*, 5265–5274 (2018). doi:10.1109/CVPR.2018.00552.
- [24] Beltagy, I., Lo, K. & Cohan, A. SciBERT: A Pretrained Language Model for Scientific Text. In *The 2019 Conference on Empirical Methods in Natural Language Processing and the 9th International Joint Conference on Natural Language Processing (EMNLP-IJCNLP 2019)*, 3615–3620 (2019). doi:10.18653/v1/D19-1371.
- [25] Grattafiori, A. *et al.* The Llama 3 Herd of Models. *CoRR* (2024). arXiv:2407.21783.
- [26] Pasińska, K. *et al.* A paraelectric–ferroelectric phase transition of an organically templated zinc oxalate coordination polymer. *Dalton Trans.* **47**, 11308–11312 (2018). doi:10.1039/C8DT02859A.
- [27] Li, C.-A. *et al.* A PEG/copper(I) halide cluster as an eco-friendly catalytic system for C–N bond formation. *Dalton Trans.* **47**, 7463–7470 (2018). doi:10.1039/C8DT01310A.
- [28] Mironov, A. V., Petříček, V., Khasanova, N. R. & Antipov, E. V. New insight on bismuth cuprates with incommensurate modulated structures. *Acta Cryst B* **72**, 395–403 (2016). doi:10.1107/S2052520616005643.
- [29] Ogunbunmi, M. O., Baranets, S., Childs, A. B. & Bobev, S. The Zintl phases AIn<sub>2</sub>As<sub>2</sub> (A = Ca, Sr, Ba): New topological insulators and thermoelectric material candidates. *Dalton Trans.* **50**, 9173–9184 (2021). doi:10.1039/D1DT01521D.
- [30] Schütt, K. T., Sauceda, H. E., Kindermans, P.-J., Tkatchenko, A. & Müller, K.-R. SchNet – A deep learning architecture for molecules and materials. *J. Chem. Phys.* **148**, 241722 (2018). doi:10.1063/1.5019779.
- [31] Choudhary, K. & DeCost, B. Atomistic Line Graph Neural Network for improved materials property predictions. *npj Comput. Mater.* **7**, 185 (2021). doi:10.1038/s41524-021-00650-1.
- [32] Louis, S.-Y. *et al.* Graph convolutional neural networks with global attention for improved materials property prediction. *Phys. Chem. Chem. Phys.* **22**, 18141–18148 (2020). doi:10.1039/D0CP01474E.
- [33] Jain, A. *et al.* Commentary: The Materials Project: A materials genome approach to accelerating materials innovation. *APL Materials* **1**, 011002 (2013). doi:10.1063/1.4812323.

- [34] Choudhary, K. *et al.* The joint automated repository for various integrated simulations (JARVIS) for data-driven materials design. *npj Comput. Mater.* **6**, 1–13 (2020). doi:10.1038/s41524-020-00440-1.
- [35] Deng, B. *et al.* CHGNet as a pretrained universal neural network potential for charge-informed atomistic modelling. *Nat. Mach. Intell.* **5**, 1031–1041 (2023). doi:10.1038/s42256-023-00716-3.
- [36] Batatia, I. *et al.* A foundation model for atomistic materials chemistry. *CoRR* (2024). arXiv:2401.00096.
- [37] Yang, H. *et al.* MatterSim: A Deep Learning Atomistic Model Across Elements, Temperatures and Pressures. *CoRR* (2024). arXiv:2405.04967.
- [38] Chanussot, L. *et al.* Open Catalyst 2020 (OC20) Dataset and Community Challenges. *ACS Catalysis* **11**, 6059–6072 (2021). doi:10.1021/acscatal.0c04525.
- [39] Tran, R. *et al.* The Open Catalyst 2022 (OC22) Dataset and Challenges for Oxide Electrocatalysts. *ACS Catalysis* **13**, 3066–3084 (2023). doi:10.1021/acscatal.2c05426.
- [40] Zhou, Q. *et al.* Learning atoms for materials discovery. *Proceedings of the National Academy of Sciences (PNAS)* **115**, E6411–E6417 (2018). doi:10.1073/pnas.1801181115.
- [41] Ryan, K., Lengyel, J. & Shatruk, M. Crystal Structure Prediction via Deep Learning. *J. Am. Chem. Soc.* **140**, 10158–10168 (2018). PMID: 29874459, doi:10.1021/jacs.8b03913.
- [42] Mikolov, T., Chen, K., Corrado, G. & Dean, J. Efficient Estimation of Word Representations in Vector Space. *CoRR* (2013). arXiv:1301.3781.
- [43] Sutskever, I., Vinyals, O. & Le, Q. V. Sequence to Sequence Learning with Neural Networks. In *Advances in Neural Information Processing Systems 27 (NIPS 2014)*, 3104–3112 (2014). arXiv:1409.3215.
- [44] Vaswani, A. *et al.* Attention Is All you Need. In *Advances in Neural Information Processing Systems 30 (NIPS 2017)*, 6000–6010 (2017). arXiv:1706.03762.
- [45] Devlin, J., Chang, M.-W., Lee, K. & Toutanova, K. BERT: Pre-training of Deep Bidirectional Transformers for Language Understanding. In *The 2019 Conference of the North American Chapter of the Association for Computational Linguistics: Human Language Technologies (NAACL-HLT 2019), Volume 1 (Long and Short Papers)*, 4171–4186 (2019). doi:10.18653/v1/N19-1423.
- [46] Radford, A., Narasimhan, K., Salimans, T. & Sutskever, I. Improving Language Understanding by Generative Pre-Training. Tech. Rep., OpenAI (2018). Online: [https://cdn.openai.com/research-covers/language-unsupervised/language\\_understanding\\_paper.pdf](https://cdn.openai.com/research-covers/language-unsupervised/language_understanding_paper.pdf).
- [47] Radford, A. *et al.* Language Models are Unsupervised Multitask Learners. Tech. Rep., OpenAI (2019). Online: [https://cdn.openai.com/better-language-models/language\\_models\\_are\\_unsupervised\\_multitask\\_learners.pdf](https://cdn.openai.com/better-language-models/language_models_are_unsupervised_multitask_learners.pdf).
- [48] Brown, T. *et al.* Language Models are Few-Shot Learners. In *Advances in Neural Information Processing Systems 33 (NeurIPS 2020)*, 1877–1901 (2020). arXiv:2005.14165.
- [49] OpenAI *et al.* GPT-4 Technical Report. *CoRR* (2024). arXiv:2303.08774.
- [50] Touvron, H. *et al.* LLaMA: Open and Efficient Foundation Language Models. *CoRR* (2023). arXiv:2302.13971.
- [51] Touvron, H. *et al.* Llama 2: Open Foundation and Fine-Tuned Chat Models. *CoRR* (2023). arXiv:2307.09288.
- [52] Tshitoyan, V. *et al.* Unsupervised word embeddings capture latent knowledge from materials science literature. *Nature* **571**, 95–98 (2019). doi:10.1038/s41586-019-1335-8.
- [53] Bommasani, R. *et al.* On the Opportunities and Risks of Foundation Models. *CoRR* (2022). arXiv:2108.07258.
- [54] Jia, C. *et al.* Scaling Up Visual and Vision-Language Representation Learning With Noisy Text Supervision. In *The 38th International Conference on Machine Learning (ICML 2021)*, vol. 139 of *Proceedings of Machine Learning Research*, 4904–4916 (2021). Online: <https://proceedings.mlr.press/v139/jia21b.html>.
- [55] Deng, J. *et al.* ImageNet: A large-scale hierarchical image database. In *The 2009 IEEE Conference on Computer Vision and Pattern Recognition (CVPR 2009)*, 248–255 (2009). doi:10.1109/CVPR.2009.5206848.
- [56] Lin, T.-Y. *et al.* Microsoft COCO: Common Objects in Context. In *The 13th European Conference on Computer Vision (ECCV 2014)*, 740–755 (2014). doi:10.1007/978-3-319-10602-1\_48.
- [57] Lewis, P. *et al.* Retrieval-Augmented Generation for Knowledge-Intensive NLP Tasks. In *Advances in Neural Information Processing Systems 33 (NeurIPS 2020)*, 9459–9474 (2020). arXiv:2005.11401.
- [58] Ramesh, A., Dhariwal, P., Nichol, A., Chu, C. & Chen, M. Hierarchical Text-Conditional Image Generation with CLIP Latents. *CoRR* (2022). arXiv:2204.06125.



- [59] Jiao, R. *et al.* Crystal Structure Prediction by Joint Equivariant Diffusion. In *Advances in Neural Information Processing Systems 36 (NeurIPS 2023)*, 17464–17497 (2023). arXiv:2309.04475.
- [60] Zeni, C. *et al.* A generative model for inorganic materials design. *Nature* (2025). doi:10.1038/s41586-025-08628-5.
- [61] Kingma, D. P. & Ba, J. Adam: A Method for Stochastic Optimization. In *The Third International Conference on Learning Representations (ICLR 2015)* (2015). arXiv:1412.6980.
- [62] Loshchilov, I. & Hutter, F. Decoupled Weight Decay Regularization. In *The Seventh International Conference on Learning Representations (ICLR 2019)* (2019). Online: <https://openreview.net/forum?id=Bkg6RiCqY7>.
- [63] Ansel, J. *et al.* PyTorch 2: Faster Machine Learning through Dynamic Python Bytecode Transformation and Graph Compilation. In *The 29th ACM International Conference on Architectural Support for Programming Languages and Operating Systems (ASPLOS 2024)*, vol. 2, 929–947 (2024). doi:10.1145/3620665.3640366.
- [64] Fey, M. & Lenssen, J. E. Fast Graph Representation Learning with PyTorch Geometric. In *The ICLR 2019 Workshop on Representation Learning on Graphs and Manifolds* (2019). arXiv:1903.02428.
- [65] Kwon, W. *et al.* Efficient Memory Management for Large Language Model Serving with PagedAttention. In *The 29th Symposium on Operating Systems Principles (SOSP 2023)*, 611–626 (2023). doi:10.1145/3600006.3613165.
- [66] Momma, K. & Izumi, F. VESTA 3 for three-dimensional visualization of crystal, volumetric and morphology data. *J. Appl. Crystallogr.* **44**, 1272–1276 (2011). doi:10.1107/S0021889811038970.
- [67] van der Maaten, L. & Hinton, G. Visualizing Data using t-SNE. *J. Mach. Learn. Res.* **9**, 2579–2605 (2008). Online: <http://jmlr.org/papers/v9/vandermaaten08a.html>.
- [68] Poličar, P. G., Stražar, M. & Zupan, B. openTSNE: A Modular Python Library for t-SNE Dimensionality Reduction and Embedding. *J. Stat. Softw.* **109**, 1–30 (2024). doi:10.18637/jss.v109.i03.
- [69] Arthur, D. & Vassilvitskii, S. k-means++: The Advantages of Careful Seeding. In *The Eighteenth Annual ACM-SIAM Symposium on Discrete Algorithms (SODA 2007)*, 1027–1035 (2007).